



Published in final edited form as:

*Cell Calcium*. 2017 September ; 66: 1–9. doi:10.1016/j.ceca.2017.05.008.

## Regulation of L-type $\text{Ca}_v1.3$ channel activity and insulin secretion by the cGMP-PKG signaling pathway

Alejandro Sandoval<sup>a</sup>, Paz Duran<sup>b</sup>, María A. Gandini<sup>c</sup>, Arturo Andrade<sup>d</sup>, Angélica Almanza<sup>e</sup>, Simon Kaja<sup>f</sup>, and Ricardo Felix<sup>b,\*</sup>

<sup>a</sup>FES Iztacala UNAM, Tlalnepantla De Baz, Mexico

<sup>b</sup>Departamento de Biología Celular, Cinvestav-IPN, Ciudad de México, Mexico

<sup>c</sup>Hotchkiss Brain Institute, University of Calgary, Calgary, AB, Canada

<sup>d</sup>Department of Biological Sciences, University of New Hampshire, Durham, NH, USA

<sup>e</sup>Dirección de Investigaciones en Neurociencias, Instituto Nacional de Psiquiatría, Ramón de la Fuente Muñiz, Ciudad de México, Mexico

<sup>f</sup>Department of Ophthalmology and Molecular Pharmacology & Therapeutics, Loyola University, Chicago, Strich School of Medicine, Maywood, IL, USA

### Abstract

cGMP is a second messenger widely used in the nervous system and other tissues. One of the major effectors for cGMP is the serine/threonine protein kinase, cGMP-dependent protein kinase (PKG), which catalyzes the phosphorylation of a variety of proteins including ion channels. Previously, it has been shown that the cGMP-PKG signaling pathway inhibits  $\text{Ca}^{2+}$  currents in rat vestibular hair cells and chromaffin cells. This current allegedly flow through voltage-gated  $\text{Ca}_v1.3$  L-type  $\text{Ca}^{2+}$  channels, and is important for controlling vestibular hair cell sensory function and catecholamine secretion, respectively. Here, we show that native L-type channels in the insulin-secreting RIN-m5F cell line, and recombinant  $\text{Ca}_v1.3$  channels heterologously expressed in HEK-293 cells, are regulatory targets of the cGMP-PKG signaling cascade. Our results indicate that the  $\text{Ca}_v\alpha_1$  ion-conducting subunit of the  $\text{Ca}_v1.3$  channels is highly expressed in RIN-m5F cells and that the application of 8-Br-cGMP, a membrane-permeable analogue of cGMP, significantly inhibits  $\text{Ca}^{2+}$  macroscopic currents and impair insulin release stimulated with high  $\text{K}^+$ . In addition, KT-5823, a specific inhibitor of PKG, prevents the current inhibition generated by 8-Br-cGMP in the heterologous expression system. Interestingly, mutating the putative phosphorylation sites to residues resistant to phosphorylation showed that the relevant PKG sites for  $\text{Ca}_v1.3$  L-type channel regulation centers on two amino acid residues, Ser793 and Ser860, located in the intracellular loop connecting the II and III repeats of the  $\text{Ca}_v\alpha_1$  pore-forming subunit of the channel. These findings unveil a novel mechanism for how the cGMP-PKG signaling pathway may regulate  $\text{Ca}_v1.3$  channels and contribute to regulate insulin secretion.

\*Corresponding author at: Departamento de Biología Celular, Cinvestav-IPN, Avenida IPN 2508, Colonia Zacatenco, Ciudad de México, CP 07360, Mexico. rfelix@cinvestav.mx (R. Felix).

### Conflict of interest

The authors declare no conflict of interest.

## Keywords

L-type channels; Cav channels; PKG; cGMP; Insulin; Rin-m5F cells

---

## 1. Introduction

Voltage-gated  $\text{Ca}^{2+}$  ( $\text{Ca}_V$ ) channels are  $\text{Ca}^{2+}$ -conducting proteins in the cell membrane that in response to a depolarization undergo a conformational change from a non-conducting state to a transiently high  $\text{Ca}^{2+}$  permeable state [1–3]. This allows extracellular  $\text{Ca}^{2+}$  to rapidly enter the cytoplasm where it serves as a second messenger to trigger a myriad of cellular responses including neurotransmitter and hormone release, muscle contraction and gene expression, among many others [1–3]. Therefore it comes as no surprise that malfunction of  $\text{Ca}_V$  channels resulting from mutation, altered expression or regulation may lead to disease [3,4].

Multiple subtypes of  $\text{Ca}^{2+}$  channel currents have been defined by physiological and pharmacological criteria. In some cell types,  $\text{Ca}^{2+}$  currents are characterized by their high voltage of activation, large conductance, and specific inhibition by antagonist drugs including dihydropyridines [1,3]. These currents that also show slow voltage-dependent inactivation are named L-type (long-lasting), are present in endocrine cells where they initiate the hormone release process, and in neurons where they are important in the integration of the synaptic input and the regulation of gene expression [1,3].

L-type  $\text{Ca}_V$  channels are multisubunit complexes formed by one of four distinct ion-conducting  $\text{Ca}_V\alpha_1$  subunits, now called  $\text{Ca}_V1.1$  to  $\text{Ca}_V1.4$ , that co-assemble with ancillary  $\text{Ca}_V\beta$ ,  $\text{Ca}_V\alpha_2\delta$ , and in some cases  $\text{Ca}_V\gamma$  subunits [1–5]. The  $\text{Ca}_V\alpha_1$  subunit comprises four homologous repeats each consisting of six transmembrane helices and a pore lining domain. These repeated domains are linked via cytoplasmic loops and flanked by intracellular N- and C-termini [1–5].  $\text{Ca}_V1.1$  and  $\text{Ca}_V1.4$  channels are predominantly expressed in skeletal muscle, pituitary cells and the retina, whereas  $\text{Ca}_V1.2$  and  $\text{Ca}_V1.3$  are broadly distributed throughout the central nervous system, endocrine cells, cardiac myocytes and sinoatrial node cells [3,7]. These channels are substrates for phosphorylation by different protein kinases, which is believed to be of substantial physiological importance, mediating the effects of several hormones and intracellular messengers [6–8].

In particular, L-type channels are regulated by a mechanism originated in the NO-cGMP-PKG signaling pathway. In rat vestibular hair cells it has been reported that NO donors inhibit the macroscopic  $\text{Ca}^{2+}$  that flows presumably through L-type of the  $\text{Ca}_V1.3$  class in a voltage-independent manner [9]. The membrane-permeant cGMP analogue 8-Br-cGMP mimicked the inhibitory action of NO donors and KT-5823, a selective inhibitor of cGMP-dependent protein kinase (PKG), prevented the inhibition of the current caused by NO donors and 8-Br-cGMP [9], supporting the idea that NO inhibits the  $\text{Ca}^{2+}$  current by the activation of the cGMP-signaling pathway.

These data agree with results obtained in chromaffin cells where application of the membrane-permeable cGMP analogue 8-pCPT-cGMP significantly decreased L-type

channel activity and disfavored catecholamine release [10–12]. Interestingly, L-type channels in these cells can be also modulated by the cAMP-PKA signaling cascade but in an opposite direction (*i.e.*, upregulation). Both PKG and PKA appear to affect  $\text{Ca}_v1.3$ , as well as  $\text{Ca}_v1.2$  channels, to the same extent both under basal conditions and in response to maximal stimulation [12]. Analogously, experimental evidence supports the idea that PKA may phosphorylate  $\text{Ca}_v1.3$  channel pore-forming  $\alpha_1$  subunit at serine residues 1743 and 1816 [13], but nothing is known regarding the phosphorylation sites of PKG.

Using patch-clamp electrophysiology, here we report for the first time that these currents are directly targeted and inhibited by the cGMP-PKG signaling cascade in insulin-secreting RIN-m5F cells. Furthermore, insulin secretion by these cells may be also affected by 8-Br-cGMP and KT-5823 application. Subsequent work using a heterologous expression system and site-directed mutagenesis identified two serine residues (Ser793 and Ser860) in the intracellular loop connecting the II and III repeats of the  $\text{Ca}_v1.3\alpha_1$  pore-forming subunit of the channel whose phosphorylation leads to down-regulation of the channel complex.

## 2. Materials and methods

### 2.1. Cell culture and transfection

The rat insulin-producing RIN-m5F cells (CRL-11605; ATCC) were grown as monolayers in RPMI 1640 medium (Sigma-Aldrich) supplemented with 10% fetal bovine serum, 110 mg/L sodium pyruvate, 2 mM L-glutamine, 100 units/L penicillin, and 100  $\mu\text{g}/\text{L}$  streptomycin. Likewise, HEK-293 cells (CRL-1573; ATCC) were grown also as monolayers in DMEM-high glucose medium (Sigma-Aldrich) supplemented with 10% fetal bovine serum, 110 mg/L sodium pyruvate, 2 mM L-glutamine, 100 U/L penicillin, and 100  $\mu\text{g}/\text{L}$  streptomycin. Cell cultures were maintained at 37 °C in 5%  $\text{CO}_2$ , and 95% air humidified atmosphere.

After splitting, HEK-293 cells were seeded at 60% confluence and one day after were transfected using the Lipofectamine Plus reagent (Invitrogen) with 1.0  $\mu\text{g}$  of each plasmid cDNA encoding L-type channel pore-forming subunit  $\text{Ca}_v1.3\alpha_1$  (GenBank™ accession number AF370009), cloned into the pcDNA6 vector (Invitrogen), and auxiliary subunits  $\text{Ca}_v\beta_3$  (M88751), and  $\text{Ca}_v\alpha_2\beta-1$  (M86621) cloned into the pcDNA3 vector (Invitrogen). For electrophysiological recording, 0.6  $\mu\text{g}$  of a plasmid encoding the green fluorescent protein (Green-Lantern; Invitrogen) was used to identify transfected cells.

### 2.2. RNA extraction, reverse transcription and PCR amplification

Total RNA was extracted from RIN-m5F cells by using TRI-zol (Invitrogen). Reverse transcription was performed using 1  $\mu\text{g}$  of total RNA by the SuperScript III first strand system for RT-PCR (Invitrogen). The sequences of the primers used for PKG amplification were 5′-AAGATTCTCATGCTCAAGGA-3′ and 5′-CAGCTCCAAGTTCTTCATGA-3′, forward and reverse, respectively.  $\beta$ -actin, used as a control, was amplified using a sense primer 5′-AAGATGACCCAGATCATGTT-3′ and an antisense primer 5′-GAGTACTTGCGCTCAGGAGG-3′ (Suppl Table S1). End-point PCR was carried out in 50  $\mu\text{l}$  (total volume) containing 5  $\mu\text{l}$  cDNA, 1 $\times$  PCR buffer, 200  $\mu\text{M}$  each deoxynucleotide

triphosphate, 200 nM each primer, 1.5 mM MgCl<sub>2</sub>, and 2.5 units of Taq DNA polymerase on a thermal cycler for 30 cycles. Denaturation, annealing and elongation were carried out at 94 °C for 45 s, 55 °C for 30 s, and 72 °C for 60 s, respectively. PCRs were performed using Taq DNA polymerase (Invitrogen) with a 200 nM concentration of each primer.

### 2.3. RNA extraction, and quantitative PCR

Total RNA was isolated from dry pellets of RIN-m5F cells stored at -80 °C using the Ambion RNaqueous4PCR kit (Applied Biosciences) according to the manufacturer's recommendations. Quantity and quality of total RNA was assessed using a spectrophotometer. cDNA was synthesized from 2 µg total RNA using the High-Capacity cDNA Reverse Transcription Kit (Applied Biosystems). Amplification efficiency was determined by reducing the template amount in the cDNA synthesis reaction to 200, 20 and 2 ng and calculated using the formula,  $Ex = (-1/\text{slope}) - 10$ , where Ex is the amplification efficiency. The quantitative polymerase chain reaction was performed using a StepOne Plus PCR System and gene-specific FAM- and VIC-labeled Taqman gene expression assays (Applied Biosystems, see Suppl. Table S2) using a total reaction volume of 20 µl, and the equivalent of 50 ng total RNA (0.5 µl) transcribed to cDNA per well. Rat β-actin was used as endogenous control. In order to obtain standard curves, genomic sequences of 200 bp length N- and C-terminal of the Taqman probe were amplified using standard PCR protocols, cloned into a pUC18 cloning vector (Fermentas) and verified by sequencing. We performed quantitative gene expression analysis and data was exported and plotted in Prism Software (GraphPad Inc). Statistical significance was determined using analysis of variance (ANOVA) with Student-Newman-Keuls *post-hoc* test.

### 2.4. Electrophysiology

Electrophysiological recordings were performed according to the whole cell variant of the patch clamp technique [14] at room temperature (~22 °C). The bath solution contained (in mM): 10 or 5 BaCl<sub>2</sub> (for RIN-m5F and HEK-293, respectively), 125 TEA-Cl, 10 HEPES, and 10 glucose (pH 7.3). Patch pipettes were filled with a solution containing (in mM): 120 CsCl, 10 HEPES, 10 EGTA, 5 MgCl<sub>2</sub>, 4 ATP, and 0.1 GTP (pH 7.3). The osmolarity was adjusted to ~280 mOsm/L and 300 mOsm/L for the internal and external solutions, respectively. Recordings were performed using an Axopatch 200 B amplifier (Molecular Devices) and filtered at 2 kHz (internal four-pole Bessel filter). Currents were acquired at a frequency of 5.71 kHz by means of a DigiData 1320A digitizer (Molecular Devices) and analyzed using the pCLAMP (Molecular Devices) and SigmaPlot (Systat) software applications. Linear capacitative currents were canceled using the amplifier and by subtraction using a P/4 protocol. Membrane capacitance ( $C_m$ ) was determined as described previously and used to normalize currents [15]. Series resistance values were typically 2–10 MΩ, and recordings where the voltage error ( $V_{er} = I_{max} \times R_s$ ) was >5 mV (at its maximal value) were not subjected to further analysis. Currents were recorded by applying 140 ms pulses, between -70 and 50 mV in the case of RIN-m5F cells and from -70 to 30 mV in the case of HEK-293 cells, in 5-mV increments from a holding potential ( $V_h$ ) of -80 mV. Current-voltage ( $I-V$ ) relationships were generated from the peak current obtained during the pulses and were fitted with an equation of the form  $I = (V_h - V_{rev}) / [1 + \exp(V_{0.5} - V_h/k)]$  where,  $I$  is the peak current density (in pA/pF) at a given  $V_h$ ,  $V_{0.5}$  is the voltage at

which half of the channels are activated,  $V_{rev}$  is the reversal potential, and  $k$  is the slope factor [16].

## 2.5. Insulin secretion

RIN-m5F cells were washed with PBS and preincubated with Krebs-Ringer buffer consisting of (in mM) 25 HEPES, 115 NaCl, 24 NaHCO<sub>3</sub>, 5 KCl, 1 MgCl<sub>2</sub>, 2.5 mM CaCl<sub>2</sub> and 0.1% BSA for 5 min at 37°C in 5% CO<sub>2</sub>, and 95% air humidified atmosphere. The preincubation buffer was removed and replaced with Krebs-Ringer buffer containing 40 mM KCl for 10 min at 37 °C. Insulin secretion was assessed by the enzyme-linked immunosorbent assay (ELISA) using the rat insulin ELISA kit (Alpco) according to the manufacturer's recommendations.

## 2.6. Site directed mutagenesis

The cDNA encoding the L-type channel pore-forming Ca<sub>v</sub>1.3α<sub>1</sub> subunit cloned into the pcDNA6 expression vector was used as a template. The point mutations were introduced with ~40-mer synthetic oligonucleotides using the Quik-Change XL-mutagenesis kit (Stratagene). Initially, single amino acid mutations changing separately two serine residues to alanine (Ser793Ala and Ser860Ala) were created. Next, a double phosphorylation mutant (DPM) was generated by mutating the Ser793Ala cDNA using the Ser860Ala primers. cDNAs of all mutant channel Ca<sub>v</sub>1.3α<sub>1</sub> subunit were sequenced on an automated sequencer (ABIPrism310; Suppl Fig. S1C).

## 2.7. In vitro phosphorylation assay

The loop connecting the II and III repeats of the Ca<sub>v</sub>1.3 WT or S793A/S860A double mutant constructs were incubated with 150 U of bovine lung PKG, Ia (Millipore) and 1 mM cGMP in kinase reaction buffer (20 mM Tris-HCl, pH 7.5, 1 mM MgCl<sub>2</sub>) in a final volume of 30 μL for 30 min at 37 °C. The reaction was stopped by adding 6 μL (6X) SDS sample buffer, and subsequently boiled for 5 min at 96 °C. Samples were separated by 15% SDS-PAGE and gel bands transferred to nitrocellulose membranes for Western blotting using a mouse anti-phosphoserine monoclonal antibody (Sigma-Aldrich; dilution 1:500).

## 2.8. Chemicals and drugs

8-Br-cGMP (Cat. # B1381), SNP (Cat. # 71778), CPTIO (Cat. # C221), and H-89 (Cat. # B1427) were obtained from Sigma-Aldrich, prepared as stock in distilled water, aliquoted and stored at -20 °C. KT5823 (Cat. # K1388) and Calyculin A (Cat. # C5552) were prepared as stock in dimethyl sulfoxide (DMSO). The final concentration of DMSO in the bath recording solution was <0.05% (vol/vol). All other chemicals were of reagent grade and obtained from different commercial sources.

### 3. Results

#### 3.1. The cGMP-PKG signaling pathway regulates native L-type Ca<sub>v</sub> channels and insulin release in RIN-m5F cells

It has been reported that L-type Ca<sub>v</sub> channels can be regulated by the NO-cGMP-PKG pathway in chromaffin cells from mouse and bovine [7,9,12], and in hair cells of the inner ear from rat and frog [11,17]. Likewise, there is growing evidence for the presence of this signaling cascade in pancreatic β-cells, though there are only a few reports concerning the action mechanism of NO in these cells [18–20].

Therefore, we first investigated the functional consequences of the cGMP-PKG pathway activation on the regulation of L-type Ca<sub>v</sub> channel activity in the insulin-secreting cell line RIN-m5F. To this end, end-point RT-PCR and real-time quantitative PCR were used as methods to analyze the expression of PKG and different subunits that compose the L-type Ca<sub>v</sub> channel complexes in the RIN-m5F cells. By using specific primers (see Suppl Table S2), conspicuous RNA signals for PKG were consistently observed in both the RIN-m5F cells and the whole mouse brain used as control tissue (Fig. 1A). In addition, given that RIN-m5F cells co-express Ca<sub>v</sub>1.2 and Ca<sub>v</sub>1.3 L-type as well as non-L-type (Ca<sub>v</sub>2.2) channels [21], we performed mRNA copy number analysis for the three pore-forming subunits of these channels, as well as two genes encoding the Ca<sub>v</sub>β auxiliary subunits. The copy number of β-actin mRNA was used as normalization control. As can be seen in Fig. 1B, Ca<sub>v</sub>1.3α<sub>1</sub> and Ca<sub>v</sub>β<sub>3</sub> were the predominant subunits in the RIN-m5F cells and were expressed about five- to nine-fold higher compared to the other corresponding subunits analyzed. Interestingly, the Ca<sub>v</sub>1.2 transcripts accounted only ~20% of the L-type channels expressed in these cells.

To assess the potential involvement of PKG in the regulation of L-type Ca<sub>v</sub> channel activity, we next analyzed the effect of 8-Br-cGMP, a membrane-permeable analogue of cGMP, on the whole-cell currents in RIN-m5F cells incubated at room temperature (~22 °C) for 10 min before electrophysiological recordings. To enhance the effects of PKG activation, this study monitored whole cell currents in the presence of 10 mM Ba<sup>2+</sup> as charge carrier, and Calyculin A, an inhibitor of protein phosphatases, which by itself do not modify Ca<sup>2+</sup> current density. In these conditions, a robust voltage-dependent inward current was observed, and according to the results in the preceding section they may be carried mostly by Ca<sub>v</sub>1.3/Ca<sub>v</sub>β<sub>3</sub> channels. The currents decayed with a slow time course ( $\tau = 31.1 \pm 2.3$  ms) and the average current density-voltage relationships (peak current amplitude normalized by  $C_m$ ) reached a maximum at about 0 mV (Fig. 2A and B). Notably, the application of 8-Br-cGMP significantly decreased the whole cell current in RIN-m5F cells to about 55% of its control value at 0 mV ( $n = 12-14$  cells). We next investigated the physiological impact of the activation of PKG by 8-Br-cGMP on L-type Ca<sub>v</sub> channel activity by assessing insulin secretion from RIN-m5F cells. Interestingly, release of insulin triggered by Ca<sup>2+</sup> influx in response to high K<sup>+</sup>-induced membrane depolarization (40 mM K<sup>+</sup>; 10 min) was significantly reduced (~20%) in cells treated with 8-Br-cGMP at a 2 mM concentration. Conversely, application of the specific PKG antagonist KT-5823 increased (~30%) insulin release triggered by depolarization with high K<sup>+</sup> (Fig. 2C). Altogether, these

data stresses the importance of L-type  $\text{Ca}_V$  channel regulation by cGMP-PKG signaling pathway for fine tuning insulin release.

### 3.2. The cGMP-PKG signaling pathway regulates recombinant L-type $\text{Ca}_V1.3$ channels

We next investigated the regulation of  $\text{Ca}_V1.3$  channels by the NO-cGMP-PKG pathway using recombinant channels in the HEK-293 cell line, a heterologous expression system that does not express endogenous  $\text{Ca}_V$  channels [15,16]. Hence, the  $\text{Ca}_V1.3\alpha_1$  channel pore-forming subunit together with the  $\text{Ca}_V\beta_3$  and the  $\text{Ca}_V\alpha_2\delta-1$  auxiliary subunits were transiently co-transfected in HEK-293 cells and electrophysiological recordings were performed 48 h after transfection. In an initial series of experiments, we confirmed the endogenous expression of PKG in the HEK-293 cells by RT-PCR experiments (Fig. 3A). Next, we evaluated the action of the nitric oxide (NO) donor sodium nitroprusside (SNP), as well as 2-(4-carboxyphenyl)-4,4,5,5-tetramethylimidazoline-1-oxyl-3-oxide (CPTIO), a specific scavenger of NO, on the whole cell  $\text{Ba}^{2+}$  currents through recombinant channels heterologously expressed in the HEK-293 cell line. The application of 100  $\mu\text{M}$  SNP significantly decreased current amplitude through recombinant  $\text{Ca}_V1.3$  channels in HEK-293 cells ( $\sim 33 \pm 5\%$ ;  $n = 14$  cells;  $P < 0.01$ ) with no significant effects on the current activation or inactivation rates (Fig. 3B). A similar decrease in current amplitude was observed after the application of 1 mM SNP. The inhibitory action of SNP (100  $\mu\text{M}$ ) on the currents was significantly reduced (to  $\sim 10 \pm 3\%$ ;  $n = 6$  cells; compared with the  $\sim 33\%$  caused by SNP alone;  $P < 0.01$ ) in the presence of CPTIO (500  $\mu\text{M}$ ). These results suggest that the currents through  $\text{Ca}_V1.3/\text{Ca}_V\beta_3/\text{Ca}_V\alpha_2\delta-1$  channels heterologously expressed in HEK-293 cells may be modulated by NO.

In order to investigate whether the current inhibition produced by NO was mediated by an increase in the levels of cGMP and the activation of PKG, we next carried out a series of experiments in the presence of 8-Br-cGMP and KT-5823, a specific inhibitor of PKG. As can be seen in Fig. 3C, the application of 0.4 and 1 mM of 8-Br-cGMP significantly decreased current amplitude through recombinant  $\text{Ca}_V1.3$  channels in HEK-293 cells ( $\sim 20$  and  $\sim 35\%$ , respectively;  $n = 3-10$  cells;  $P < 0.01$ ) with no significant effects on the current activation or inactivation rates. Interestingly, co-application of 0.4 mM 8-Br-cGMP and KT-5823 (1 or 30  $\mu\text{M}$ ) significantly prevented the inhibitory action of 8-Br-cGMP (Fig. 3C). These results suggest that the effects induced by 8-Br-cGMP on the  $\text{Ca}_V1.3/\text{Ca}_V\beta_3/\text{Ca}_V\alpha_2\delta-1$  channel currents could be mediated by the activation of PKG.

Superimposed traces in Fig. 4A show that 8-Br-cGMP at a concentration of 1 mM significantly decreased the whole cell current after  $\sim 10$  min of incubation (to  $\sim 52\%$  of the control value at  $-30$  mV;  $n = 22$  cells;  $P < 0.01$ ), mimicking to some extent the action of SNP. Boltzmann fitting shown in the  $I-V$  relationships (Fig. 4B) indicated that the  $V_{0.5}$  of current activation was slightly shifted (by  $< 5$  mV) in the presence of 8-Br-cGMP and changes in the slope parameter were also not statistically significant. On the other hand, the inhibitory effect of 8-Br-cGMP on the currents was fully prevented by the use of the PKG inhibitor KT-5823 (10  $\mu\text{M}$ ), indicating that the inhibition produced by 8-Br-cGMP is mediated by the activation of the PKG.

### 3.3. Identification of the sites of cGMP-dependent phosphorylation in the $\text{Ca}_v1.3\alpha_1$ subunit

Having shown that  $\text{Ca}_v1.3$  channel modulation by NO implies the participation of PKG, we next searched for the presence of the consensus sequence for PKG phosphorylation in the pore-forming  $\text{Ca}_v\alpha_1$  channel subunit sequence using the database publicly available at the URL <http://gps.biocuckoo.org/>. We identified several sites in the  $\text{Ca}_v1.3\alpha_1$  sequence as potential PKG substrates with high score, including Thr455, Ser697, Ser793, Ser860 and Ser1581 (Suppl Fig. S1A). The first site was located in the I–II loop of the  $\text{Ca}_v\alpha_1$  subunit, other three were present in the II–III loop, and one more in the C-terminal of the protein. However, serine residues 793 and 860 were identified as the main sites of PKG phosphorylation because they were conserved among species and exhibited the highest scores (Suppl Fig. S1B).

To determine whether these sites were indeed phosphorylated by PKG, we next generated two individual and one double mutation in which these serine residues were substituted with alanines by site-directed mutagenesis, and then we tested them in whole cell patch-clamp recordings. First, a construct encoding the full-length  $\text{Ca}_v1.3\alpha_1$  along with the auxiliary subunits ( $\text{Ca}_v\beta_3/\text{Ca}_v\alpha_2\delta-1$ ) cDNAs were transiently transfected into HEK-293 cells. It is worth mentioning that the recombinant channels showed satisfactory levels of expression and generated typical current waveforms expected from L-type  $\text{Ca}_v1.3$  channels. Unexpectedly, current density was larger in cells transfected with  $\text{Ca}_v1.3$  channels harboring the Ser793 mutation at most of the voltages tested (Fig. 5A), but no differences in current kinetics were evident. The corresponding  $I-V$  relationship showed a significant  $\sim 1.5$ -fold increase in current density in the control, however in cells treated with 8-Br-cGMP (Fig. 5B) there was a decrease similar to that observed for the wild-type channels.

Given that PKG, PKA and PKC phosphorylation sites are distinct, these data suggest that the cGMP-PKG pathway may be already active at basal resting conditions, and down-regulate the channels by phosphorylating the  $\text{Ca}_v1.3\alpha_1$  at position Ser793. However, it has been also recognized that the existence of distinct phosphorylation sites for PKG and PKA does not rule out the possibility that they may mutually interfere on channel gating [7]. For this reason, we next decided to test the actions of the PKA blocker H-89 on the whole-cell currents through wild-type channels. It is acknowledged that the cGMP-PKG-mediated down-regulation of  $\text{Ca}_v1.3$  L-type channels may exert an opposite action to the cAMP/PKA-mediated up-regulation. In this scenario, we hypothesized that if serine residue at position 793 was a regulatory target of PKA, then currents through wild-type channels were going to be increased when PKA activity was blocked by H-89. However, the application of H-89 (100 nM) significantly decreased current density ( $\sim 22 \pm 6\%$  at  $-30$  mV;  $n = 5$ ,  $P = 0.05$ ; Suppl. Fig. S2B) through wild-type channels, indicating that indeed PKA phosphorylate different serine sites of the  $\text{Ca}_v1.3\alpha_1$  subunit. On the other hand, the second and most convincing evidence in favor that the  $\text{Ca}_v1.3$  channels are phosphorylated at rest by the cGMP-PKG pathway comes from experiments using the PKG blocker KT-5823. As can be seen in Fig. 4B, application of KT-5823 alone causes a significant increase in current density through wild-type  $\text{Ca}_v1.3$  channels which is similar to the up-regulation observed for the Ser793Ala channel currents (Fig. 5A and B).



In sharp contrast, substitution of serine 860 by alanine produced mutant  $\text{Ca}_V1.3$  channels refractory to modulation by PKG (Fig. 5C and D), supporting the unique importance of this amino acid residue in the  $\text{Ca}_V1.3\alpha_1$  channel subunit as a direct regulatory target of PKG. Last, as observed in currents recorded through Ser860Ala mutant  $\text{Ca}_V1.3$  channels, the magnitude of the currents through  $\text{Ca}_V1.3$  harboring the double phosphorylation mutation was not different from that observed with the wild type channels, both in the absence and presence of 8-Br-cGMP (Fig. 6). As in all cases, no differences in voltage dependence or current kinetics were also apparent. These data are consistent with the results of an *in vitro* phosphorylation assay in which a HIS fusion protein containing the region of interest (the loop connecting the II and III repeats in  $\text{Ca}_V1.3\alpha_1$ ) was generated using the pRSET A expression vector (Invitrogen), and then expressed in BL21 cells. Western blot analysis using an anti-phosphoserine monoclonal antibody showed that PKG phosphorylated the wild-type II–III loop of the  $\text{Ca}_V1.3\alpha_1$  HIS fusion protein, whereas the double phosphorylation mutant construct displayed negligible levels of phosphorylation (Suppl. Fig. S2C).

#### 4. Discussion

L-type  $\text{Ca}_V$  channels are regulatory targets for a range of second messengers in different tissues. These modulatory effects are generally mediated through G protein signaling cascades linked to protein kinases [3,6,7,22–24]. In this context, functional studies in rat vestibular hair cells and chromaffin cells have documented an inhibitory effect of PKG on L-type  $\text{Ca}_V1.3$  channels [7,11,12]. These observations raised the possibility that  $\text{Ca}_V1.3$  channel activity in other cell lines and tissues, for example insulin-secreting cells, may be also inhibited by PKG. In this report, we present electrophysiological observations supporting the view that a membrane-permeable analogue of cGMP may effectively modulate L-type  $\text{Ca}_V$  channels through classical PKG signaling in the clonal RIN-m5F cell line. Consistent with this idea, blockade of PKG using a specific inhibitor attenuated the ability of 8-Br-cGMP to inhibit L-type  $\text{Ca}_V$  channels in the RIN-m5F cells. These results are the first to suggest that L-type channels in insulin-secreting cells are directly targeted by cGMP signaling through PKG (Fig. 7).

Given that in clonal insulin-secreting cell lines and pancreatic islets from different species, L-type  $\text{Ca}_V$  channels are coupled to glucose-stimulated insulin secretion [25], it was expected that PKG-mediated channel inhibition may also affect hormone release. The present study reveals that indeed this regulation significantly reduced insulin secretion triggered by  $\text{Ca}^{2+}$  influx in response to high  $\text{K}^+$ -induced membrane depolarization, demonstrating the importance of L-type channel regulation by cGMP-PKG cascade for fine tuning hormone release. Here it is worth mentioning that insulin secretion in mice depends mainly on the activity of  $\text{Ca}_V1.2$  channels, but in rats and humans it has been shown that it relies mainly on the activity of the  $\text{Ca}_V1.3$  channels [25–27].

Previous studies have also documented the regulation of L-type  $\text{Ca}_V1.3$  channels by post-translational modifications including phosphorylation by different protein kinases. For example, it has been observed that protein kinase C (PKC) phosphorylates  $\text{Ca}_V1.3\alpha_1$  channel subunit at serine residue 81 located at the N-terminal of the protein and that this

phosphorylation decreases  $\text{Ca}^{2+}$  current amplitude in tsA201 cells expressing recombinant channels [28]. On the other hand, phosphorylation of  $\text{Ca}_v1.3$  channels by cAMP-dependent protein kinase (PKA) results in an increase in current density through native and recombinant channels [12,29,30].

Interestingly, Carbone and colleagues (2012) determined in chromaffin cells that L-type  $\text{Ca}_v1.3$  and  $\text{Ca}_v1.2$  channels are regulated with the same effectiveness, but with opposite effects, by PKA and PKG phosphorylation. Hence, phosphorylation by PKA causes an increase in  $\text{Ca}^{2+}$  currents, whereas PKG phosphorylation results in a decrease in  $\text{Ca}^{2+}$  current amplitude. These authors reported that the effects of these protein kinases on channel activity are independent and may also participate in the regulation of catecholamine release. However, the specific sites of such phosphorylation events were not established [7,9,12].

In agreement with these previous reports, in the present work we observed a down-regulation of  $\text{Ca}_v1.3$  channel activity (specifically of the  $\text{Ca}_v1.3_{42A}$  isoform) by PKG in HEK-293 cells, and that this regulation is mediated by phosphorylation in two serine residues located at position 793 and 860 in the intracellular loop that connects the II and III repeated domains of the pore-forming  $\text{Ca}_v\alpha_1$  subunit of the channel complex (Fig. 6). These might actually be phosphorylated in the cellular context, as no apparent changes in the electrophysiological properties of the mutant channels were observed.

An interesting finding of our work is that PKG seems to affect  $\text{Ca}_v1.3$  differentially depending on the phosphorylation site. As mentioned earlier, alanine substitution of  $\text{Ca}_v\alpha_1.3$  serine at position 860 fully prevented the PKG-mediated inhibition consistent with the premise that phosphorylation at this residue site may be responsible for the decrease in  $\text{Ca}_v1.3$  current amplitude after exposure to 8-Br-cGMP and Calyculin A. As mentioned earlier, Calyculin A by itself does not modify current density (Suppl Fig. S2A). Interestingly however, current density in basal conditions was larger in cells transfected with the Ser793Ala mutant channels, which represented an indication that the cGMP-PKG pathway may be active at basal resting conditions, in agreement with previous reports [12], and down-regulate the channels by phosphorylating the  $\text{Ca}_v1.3\alpha_1$  subunit at this serine residue. In support of this interpretation, application of the PKG blocker KT-5823 caused an increase in current density through wild-type  $\text{Ca}_v1.3$  channels similar to the up-regulation observed in the case of the Ser793Ala mutant channels. In this scenario, a concerted action of the two phosphorylation sites might have a cumulative effect when both sites are phosphorylated to produce maximal values of L-type currents inhibition.

It should be mentioned here that previous studies have shown differential effects on several  $\text{Ca}_v$  channels by the NO-cGMP-PKG signaling pathway. These reports suggest a down-regulation of the N-type  $\text{Ca}_v$  channels in human neuroblastoma cells IMR32 [31], and in dorsal root ganglia neurons [32]. Likewise, it has been observed that NO donors decrease  $\text{Ca}^{2+}$  currents through T-type channels in rat cerebral arterial smooth muscle cells [33], and P/Q-type  $\text{Ca}_v$  channels in rat cortical neurons [34].

However, in cortical neurons the activation of the NO-cGMP-PKG cascade had no effect on currents through N- and L-type channels [34]. In addition, it has been reported also that

activation of the NO signaling cascade actually enhances L- and P/Q-type current in mouse neurons of the medial nucleus of the trapezoid body [35]. Though the reason for these discrepancies are presently unknown, they may lie in the fact that some NO effects are mediated via cGMP, but some others depend on the ability NO to generate free radicals or produce peroxynitrite leading to protein S-nitrosylation or nitrotyrosination [36]. Indeed, redox-modulation of L-type channels has been reported in cardiac myocytes, hippocampal neurons and vestibular hair cells [11,37,38]. However, in our experiments this may not be the case because the inhibitory effect of the NO donor SNP was almost fully blocked by the NO scavenger CPTIO. In addition, it should be further noted that  $\text{Ca}_v1.3$  channels are associated with  $\text{Ca}_v\beta$  and  $\text{Ca}_v\alpha_2\delta$  auxiliary subunits which may also be subject to post-translational modifications. In line with this, previous studies have shown that the regulation of L-type  $\text{Ca}_v1.2$  channels by PKG depends also on phosphorylation of the  $\text{Ca}_v\beta_2$  auxiliary subunit [25]. This finding could help explaining the variations observed regarding the regulation of L-type  $\text{Ca}_v$  channels by PKG.

In all, the results obtained in the present work show that the repertoire of PKG down-regulation of L-type  $\text{Ca}^{2+}$  channels may extend to  $\text{Ca}_v1.3$  channels in both a heterologous system and in a cellular model that natively expresses these channels, and also show additional evidence of the functional effect this regulation may have on hormone secretion. By using a site-directed mutagenesis approach we have pinpointed the residues within the  $\text{Ca}_v1.3\alpha_1$  pore-forming subunit, which are modulated by the cGMP-PKG signaling pathway. Likewise, given the low-threshold of activation and slow rate of inactivation of  $\text{Ca}_v1.3$  channels, they could carry sufficient inward current at subthreshold potentials to activate  $\text{K}^+$  channels which contribute to determine the membrane resting potential, as well as the action potential shape and frequency during spontaneous firing or sustained depolarizations [39,40]. Therefore, the findings described here also suggest that PKG phosphorylation could play important roles in the regulation of numerous cellular processes.

## Supplementary Material

Refer to Web version on PubMed Central for supplementary material.

## Acknowledgments

This work was supported by funds from Conacyt (grant 221660) to RF; R00MH099405 to AA. We thank Mercedes Urban for expert technical assistance. Doctoral fellowship from Conacyt to PD is gratefully acknowledged. Additional support was provided by the Dr. John P. and Therese Mulcahy Endowed Professorship in Ophthalmology to SK.

## References

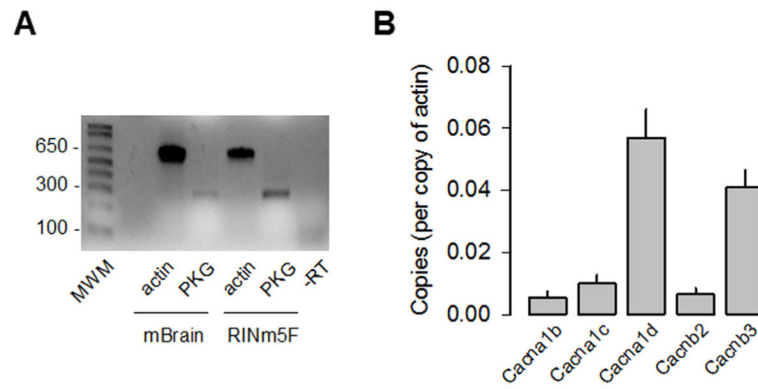
1. Gandini MA, Sandoval A, Felix R. Patch-clamp recording of voltage-sensitive  $\text{Ca}^{2+}$  channels. Cold Spring Harb Protoc. 2014; 2014:325–329. References.
2. Catterall WA. Voltage-gated calcium channels. Cold Spring Harb Perspect Biol. 2011; 3:a003947. [PubMed: 21746798]
3. Zamponi GW, Striessnig J, Koschak A, Dolphin AC. The physiology pathology, and pharmacology of voltage-gated calcium channels and their future therapeutic potential. Pharmacol Rev. 2015; 67:821–870. [PubMed: 26362469]
4. Felix R. Calcium channelopathies. Neuromol Med. 2006; 8:307–318.

5. Dolphin AC. Voltage-gated calcium channels and their auxiliary subunits: physiology and pathophysiology and pharmacology. *J Physiol.* 2016; 594:5369–5390. [PubMed: 27273705]
6. Felix R. Molecular regulation of voltage-gated  $\text{Ca}^{2+}$  channels. *J Recept Signal Transduct Res.* 2005; 25:57–71. [PubMed: 16149767]
7. Vandael DH, Mahapatra S, Calorio C, Marcantoni A, Carbone E.  $\text{Ca}_v$  1.3 and  $\text{Ca}_v$  1.2 channels of adrenal chromaffin cells: emerging views on cAMP/cGMP-mediated phosphorylation and role in pacemaking. *Biochim Biophys Acta.* 2013; 1828:1608–1618. [PubMed: 23159773]
8. Nafzger S, Rougier JS. Calcium/calmodulin-dependent serine protein kinase CASK modulates the L-type calcium current. *Cell Calcium.* 2017; 61:10–21. [PubMed: 27720444]
9. Carabelli V, D'Ascenzo M, Carbone E, Grassi C. Nitric oxide inhibits neuroendocrine  $\text{Ca}_v$  1 L-channel gating via cGMP-dependent protein kinase in cell-attached patches of bovine chromaffin cells. *J Physiol.* 2002; 541:351–366. [PubMed: 12042344]
10. Schwarz PM, Rodriguez-Pascual F, Koesling D, Torres M, Förstermann U. Functional coupling of nitric oxide synthase and soluble guanylyl cyclase in controlling catecholamine secretion from bovine chromaffin cells. *Neuroscience.* 1998; 82:255–265. [PubMed: 9483518]
11. Almanza A, Navarrete F, Vega R, Soto E. Modulation of voltage-gated  $\text{Ca}^{2+}$  current in vestibular hair cells by nitric oxide. *J Neurophysiol.* 2007; 97:1188–1195. [PubMed: 17182910]
12. Mahapatra S, Marcantoni A, Zuccotti A, Carabelli V, Carbone E. Equal sensitivity of  $\text{Ca}_v$  1.2 and  $\text{Ca}_v$  1.3 channels to the opposing modulations of PKA and PKG in mouse chromaffin cells. *J Physiol.* 2012; 590:5053–5073. [PubMed: 22826131]
13. Ramadan O, Qu Y, Wadgaonkar R, Baroudi G, Karnabi E, Chahine M, Boutjdir M. Phosphorylation of the consensus sites of protein kinase A on alpha1D L-type calcium channel. *J Biol Chem.* 2009; 284:5042–5049. [PubMed: 19074150]
14. Hamill OP, Marty A, Neher E, Sakmann B, Sigworth FJ. Improved patch-clamp techniques for high-resolution current recording from cells and cell-free membrane patches. *Pflugers Arch.* 1981; 391:85–100. [PubMed: 6270629]
15. Avila G, Sandoval A, Felix R. Intramembrane charge movement associated with endogenous  $\text{K}^+$  channel activity in HEK-293 cells. *Cell Mol Neurobiol.* 2004; 24:317–330. [PubMed: 15206817]
16. Yasuda T, Chen L, Barr W, McRory JE, Lewis RJ, Adams DJ, Zamponi GW. Auxiliary subunit regulation of high-voltage activated calcium channels expressed in mammalian cells. *Eur J Neurosci.* 2004; 20:1–13. [PubMed: 15245474]
17. Lv P, Rodriguez-Contreras A, Kim HJ, Zhu J, Wei D, Choong-Ryoul S, Eastwood E, Mu K, Levic S, Song H, Yevgeniy PY, Smith PJ, Yamoah EN. Release and elementary mechanisms of nitric oxide in hair cells. *J Neurophysiol.* 2010; 103:2494–2505. [PubMed: 20220083]
18. Tejedo JR, Ramirez R, Cahuana GM, Rincon P, Sobrino F, Bedoya FJ. Evidence for involvement of c-Src in the anti-apoptotic action of nitric oxide in serum-deprived RINm5F cells. *Cell Signal.* 2001; 13:809–817. [PubMed: 11583916]
19. Tejedo JR, Cahuana GM, Ramirez R, Esbert M, Jimenez J, Sobrino F, Bedoya FJ. Nitric oxide triggers the phosphatidylinositol 3-kinase/Akt survival pathway in insulin-producing RINm5F cells by arousing Src to activate insulin receptor substrate-1. *Endocrinology.* 2004; 145:2319–2327. [PubMed: 14764634]
20. Bedoya FJ, Salguero-Aranda C, Cahuana GM, Tapia-Limonchi R, Soria B, Tejedo JR. Regulation of pancreatic beta-cell survival by nitric oxide: clinical relevance. *Islets.* 2012; 4:108–118. [PubMed: 22614339]
21. Gandini MA, Sandoval A, González-Ramírez R, Mori Y, de Waard M, Felix R. Functional coupling of Rab3-interacting molecule 1 (RIM1) and L-type  $\text{Ca}^{2+}$  channels in insulin release. *J Biol Chem.* 2011; 286:15757–15765. [PubMed: 21402706]
22. Dai S, Hall DD, Hell JW. Supramolecular assemblies and localized regulation of voltage-gated ion channels. *Physiol Rev.* 2009; 89:411–452. [PubMed: 19342611]
23. Huang J, Zamponi GW. Regulation of voltage gated calcium channels by GPCRs and post-translational modification. *Curr Opin Pharmacol.* 2016; 32:1–8. [PubMed: 27768908]
24. Altier C, Zamponi GW. Signaling complexes of voltage-gated calcium channels and G protein-coupled receptors. *J Recept Signal Transduct Res.* 2008; 28:71–81. [PubMed: 18437631]

25. Yang SN, Berggren PO. The role of voltage-gated calcium channels in pancreatic beta-cell physiology and pathophysiology. *Endocr Rev.* 2006; 27:621–676. [PubMed: 16868246]
26. Yang G, Shi Y, Yu J, Li Y, Yu L, Welling A, Hofmann F, Striessnig J, Juntti-Berggren L, Berggren PO, Yang SN.  $\text{Ca}_V$  1.2 and  $\text{Ca}_V$  1.3 channel hyperactivation in mouse islet beta cells exposed to type 1 diabetic serum. *Cell Mol Life Sci.* 2015; 72:1197–1207. [PubMed: 25292336]
27. Zuccotti A, Clementi S, Reinbothe T, Torrente A, Vandael DH, Pirone A. Structural and functional differences between L-type calcium channels: crucial issues for future selective targeting. *Trends Pharmacol Sci.* 2011; 32:366–375. [PubMed: 21450352]
28. Baroudi G, Qu Y, Ramadan O, Chahine M, Boutjdir M. Protein kinase C activation inhibits  $\text{Ca}_V$  1.3 calcium channel at NH<sub>2</sub>-terminal serine 81 phosphorylation site. *Am J Physiol Heart Circ Physiol.* 2006; 291:H1614–H1622. [PubMed: 16973824]
29. Qu Y, Baroudi G, Yue Y, El-Sherif N, Boutjdir M. Localization and modulation of  $\alpha$ 1D ( $\text{Ca}_V$ 1.3) L-type Ca channel by protein kinase. *Am J Physiol Heart Circ Physiol.* 2005; 288:H2123–H2130. [PubMed: 15615842]
30. Marshall MR, Clark JP 3rd, Westenbroek R, Yu FH, Scheuer T, Catterall WA. Functional roles of a C-terminal signaling complex of  $\text{Ca}_V$  1 channels and A-kinase anchoring protein 15 in brain neurons. *J Biol Chem.* 2011; 286:12627–12639. [PubMed: 21224388]
31. D’Ascenzo M, Martinotti G, Azzena GB, Grassi C. cGMP/protein kinase G-dependent inhibition of N-type  $\text{Ca}^{2+}$  channels induced by nitric oxide in human neuroblastoma IMR32 cells. *J Neurosci.* 2002; 22:7485–7492. [PubMed: 12196571]
32. Yoshimura N, Seki S, de Groat WC. Nitric oxide modulates  $\text{Ca}^{2+}$  channels in dorsal root ganglion neurons innervating rat urinary bladder. *J Neurophysiol.* 2001; 86:304–311. [PubMed: 11431511]
33. Harraz OF, Brett SE, Welsh DG. Nitric oxide suppresses vascular voltage-gated T-type  $\text{Ca}^{2+}$  channels through cGMP/PKG signaling. *Am J Physiol Heart Circ Physiol.* 2014; 306:H279–H285. [PubMed: 24240871]
34. Petzold GC, Scheibe F, Braun JS, Freyer D, Priller J, Dirnagl U, Dreier JP. Nitric oxide modulates calcium entry through P/Q-type calcium channels and N-methyl-D-aspartate receptors in rat cortical neurons. *Brain Res.* 2005; 1063:9–14. [PubMed: 16274675]
35. Tozer AJ, Forsythe ID, Steinert JR. Nitric oxide signalling augments neuronal voltage-gated L-type ( $\text{Ca}_V$  1) and P/Q-type ( $\text{Ca}_V$  2.1) channels in the mouse medial nucleus of the trapezoid body. *PLoS One.* 2012; 7:e32256. [PubMed: 22389692]
36. Hess DT, Stamler JS. Regulation by S-nitrosylation of protein post-translational modification. *J Biol Chem.* 2012; 287:4411–4418. [PubMed: 22147701]
37. Campbell DL, Stamler JS, Strauss HC. Redox modulation of L-type calcium channels in ferret ventricular myocytes. Dual mechanism regulation by nitric oxide and S-nitrosothiols. *J Gen Physiol.* 1996; 108:277–293. [PubMed: 8894977]
38. Tjong YW, Jian K, Li M, Chen M, Gao TM, Fung ML. Elevated endogenous nitric oxide increases  $\text{Ca}^{2+}$  flux via L-type  $\text{Ca}^{2+}$  channels by S-nitrosylation in rat hippocampal neurons during severe hypoxia and in vitro ischemia. *Free Radic Biol Med.* 2007; 42:52–63. [PubMed: 17157193]
39. Lipscombe D, Helton TD, Xu W. L-type calcium channels: the low down. *J Neurophysiol.* 2004; 92:2633–2641. [PubMed: 15486420]
40. Vandael DH, Marcantoni A, Carbone E.  $\text{Ca}_V$  1.3 channels as key regulators of neuron-like firings and catecholamine release in chromaffin cells. *Curr Mol Pharmacol.* 2015; 8:149–161. [PubMed: 25966692]

## Appendix A. Supplementary data

Supplementary data associated with this article can be found, in the online version, at <http://dx.doi.org/10.1016/j.ceca.2017.05.008>.

**Fig. 1.**

Expression of PKG and Ca<sub>v</sub> channel subunits in RIN-m5F cells. A) RT-PCR analysis of PKG cDNA expression in RIN-m5F cells. Total RNA from mouse whole brain was used as a positive control. Actin was used as an internal control. Primer sequences are indicated in Supplemental Table S1. B) Levels of different Ca<sub>v</sub> channel subunit mRNAs expressed in RIN-m5F cells estimated from gene quantitative RT-PCR data and expressed as a number of copies of  $\beta$ -actin mRNA expression.

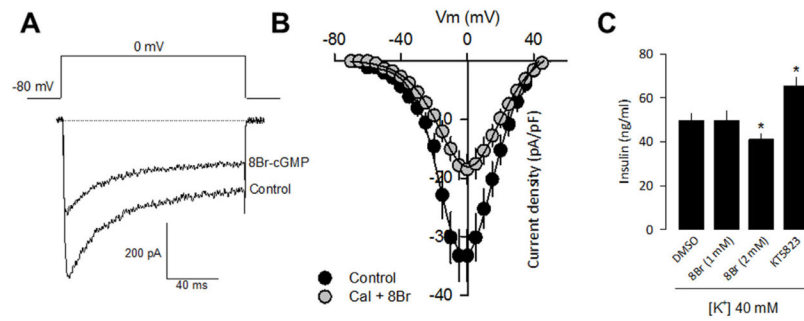


**Fig. 2.**

PKG inhibit L-type  $\text{Ca}_V$  channels in RIN-m5F cells and contributes to determine insulin secretion. A) Representative traces of  $\text{Ba}^{2+}$  currents ( $I_{\text{Ba}}$ ) through  $\text{Ca}^{2+}$  channels in RIN-m5F cells in the control condition and after 8-Br-cGMP (1 mM) application. B) Average current density-voltage relationships for  $I_{\text{Ba}}$  recorded from RIN-m5F cells in the absence and presence of 8-Br-cGMP (1 mM). C) High  $\text{K}^+$ -induced insulin secretion from RIN-m5F cells in the absence and the presence of 8-Br-cGMP as indicated. RIN-m5F cells were incubated with KRB buffer containing 40 mM KCl. Insulin content in the supernatants was measured by ELISA. The mean  $\pm$  S.E. of four independent experiments is shown.

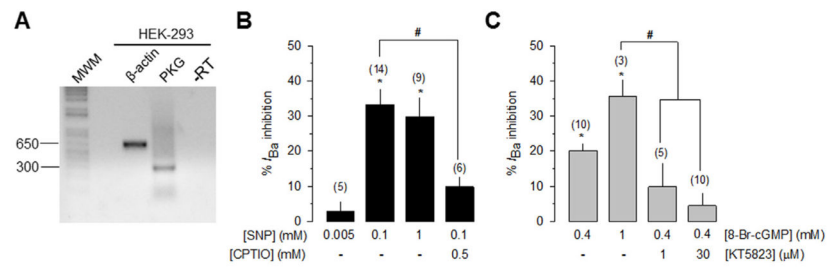


**Fig. 3.**

The NO-cGMP-PKG pathway inhibited recombinant L-type  $Ca_V$  1.3 channel activity. A) RT-PCR analysis of PKG cDNA expression in the HEK-293 cell line. Actin was used as an internal control. Primer sequences are indicated in Supplemental Table S1. B) Bar chart of the percentage inhibition  $\pm$  S.E. of  $I_{Ba}$  measured with test pulses to  $-30$  mV at different concentrations of SNP alone, or after  $500 \mu\text{M}$  CPTIO application. The number of recorded cells is indicated in parenthesis. C) Comparison of the of the percentage inhibition  $\pm$  S.E. of  $I_{Ba}$  measured with test pulses to  $-30$  mV at different concentrations of 8-Br-cGMP alone or in combination of KT-5823, as indicated.



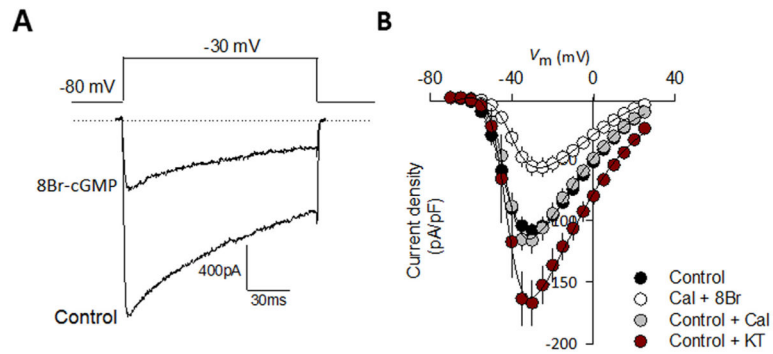


**Fig. 4.**

PKG activation modifies current density through recombinant L-type  $\text{Ca}_V$  1.3 channels. A) Representative superimposed current traces recorded in HEK-293 cells expressing  $\text{Ca}_V$  1.3/ $\text{Ca}_V$   $\alpha_2$   $\delta$ -1/ $\text{Ca}_V$   $\beta_3$  channels in the absence and presence of 8-Br-cGMP (1 mM). Currents were evoked by 140-ms depolarizing pulses from a  $V_h$  of  $-80$  to  $-30$  mV. B) Average current density-voltage relationships for  $I_{Ba}$  recorded from HEK-293 cells expressing  $\text{Ca}_V$  1.3/ $\text{Ca}_V$   $\alpha_2$   $\delta$ -1/ $\text{Ca}_V$   $\beta_3$  channels in the absence and presence of 8-Br-cGMP (1 mM), Calyculin (10 nM) and KT-5823 (10  $\mu\text{M}$ ), as indicated.

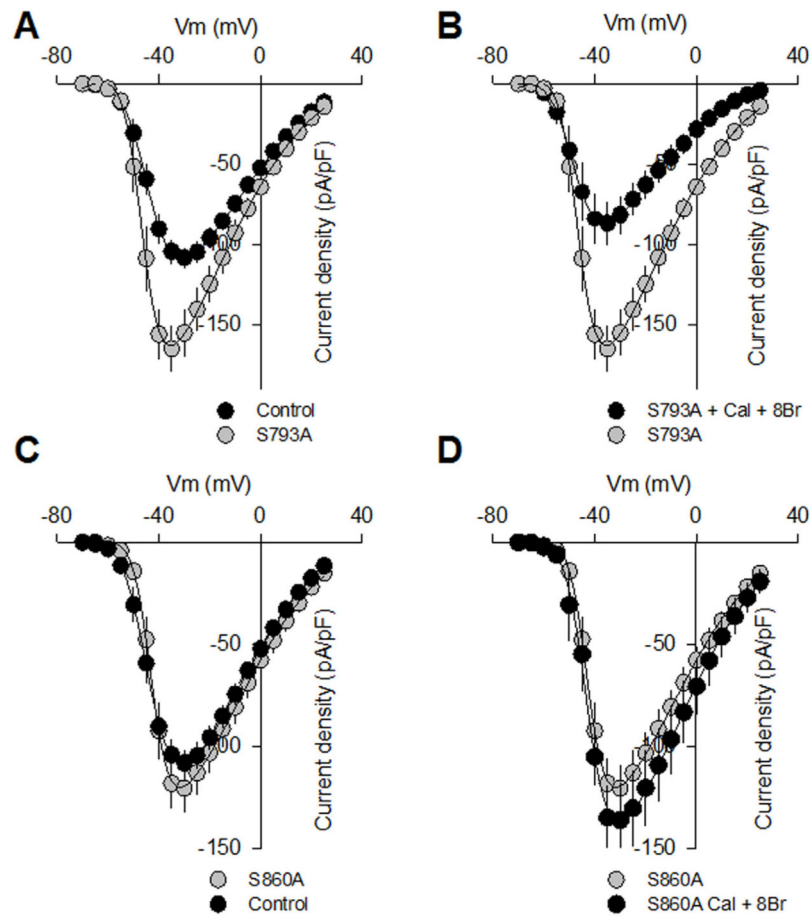


**Fig. 5.** Mutation of two serine residues (S763 and S860) to delete PKG-mediated phosphorylation sites in the  $\text{Ca}_v 1.3\alpha_1$  subunit alters channel functional expression. A) Average current density-voltage relationships for  $I_{\text{Ba}}$  recorded from HEK-293 cells expressing the wild-type  $\text{Ca}_v 1.3$  channel and its mutant variant (Ser793Ala) in the control condition and after incubation with 1 mM 8- Br-cGMP plus 10 nM Calyculin A (B).  $I_{\text{Ba}}$  density was calculated at a series of test pulses applied from a  $V_h$  of  $-80$  mV in 5 mV steps between  $-70$  and 30 mV. C) Average current density-voltage relationships for  $I_{\text{Ba}}$  recorded from HEK-293 cells expressing the wild-type  $\text{Ca}_v 1.3$  channel and its mutant variant (Ser860Ala) in the control condition and after incubation with 1 mM 8- Br-cGMP plus 10 nM Calyculin A (D).

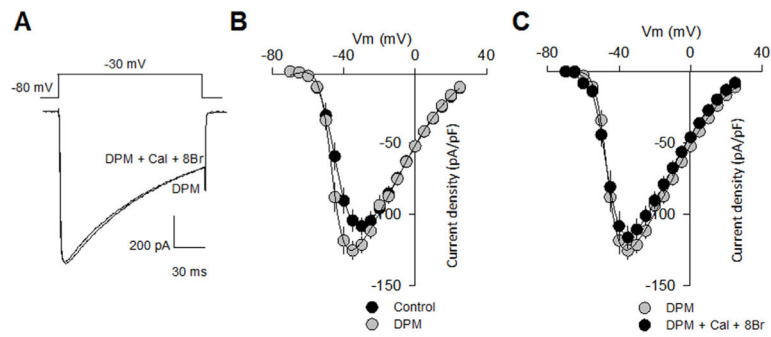


**Fig. 6.** Phosphorylation at sites S763 and S860 of Ca<sub>v</sub> 1.3α<sub>1</sub> subunit influences channel functional expression. A) Representative traces of Ba<sup>2+</sup> currents recorded from HEK-293 cells expressing DPM mutant channels in absence and presence of 8-Br-cGMP (1 mM) plus 10 nM Calyculin A. B) Average current density-voltage relationships for I<sub>Ba</sub> from HEK-293 cells expressing the wild-type Ca<sub>v</sub> 1.3 channel and its double phosphorylation mutant (DPM) variant in the control condition and after incubation with 1 mM 8-Br-cGMP plus 10 nM Calyculin A. C) I<sub>Ba</sub> density was calculated at a series of test pulses applied from a V<sub>h</sub> of -80 mV in 5 mV steps between -70 and 30 mV.

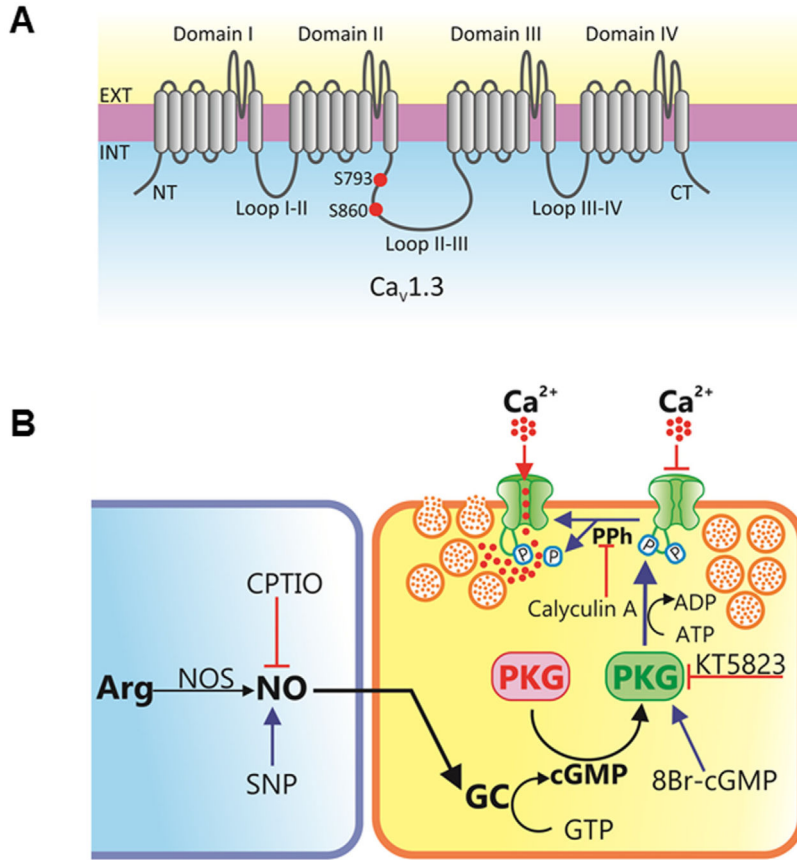


**Fig. 7.** Schematic overview of the mechanisms involved in PKG-induced regulation of L-type  $\text{Ca}_V$  channel activity and insulin secretion. A) The L-type channel complex is composed of the pore-forming  $\text{Ca}_V \alpha_1$  and auxiliary subunits ( $\text{Ca}_V \alpha_2 \delta$ ,  $\text{Ca}_V \beta$ , and  $\text{Ca}_V \gamma$ ). The pore-forming  $\text{Ca}_V \alpha_1$  subunits consist of four transmembrane domains (I–IV) and the linker joining II and III encompasses the putative PKG phosphorylation sites (S793 and S860). B) NO is synthesized by the enzyme NO synthase (NOS) through the oxidation of L-arginine to NO and L-citrulline, with the assistance of cofactors. NO endogenously produced by NOS or released from exogenously applied NO donors (sodium nitroprusside, SNP) activates NO-sensitive guanylate cyclase (GC) leading to increased synthesis of cGMP which activates PKG. The protein kinase catalyzes the phosphorylation of the L-type  $\text{Ca}_V$  channels which cause a decrease in  $\text{Ca}^{2+}$  influx through the cell membrane resulting in reduced release of insulin in RIN-m5F cells. The inhibitory action of PKG is blocked by the selective inhibitor KT-5823 and terminated by protein phosphatases (PPh). Calyculin A, is a serine/threonine phosphatase inhibitor.